Wireless Pers Commun (2015) 85:809–824
DOI 10.1007/s11277-015-2810-7

Performance Enhancement of OFDM-Based Systems Using Improved Parametric Linear Combination Pulses

Cesar A. Azurdia-Meza[1] · Hernán F. Arraño[1] · Claudio Estevez[1] · Ismael Soto[2]

Published online: 24 June 2015

Abstract As the demand for better performance increases in next-generation networks, such as 5G technologies, more efficient modulation techniques are required. In this work, we evaluate the performance of the improved parametric linear combination pulses (IPLCP) in orthogonal frequency division multiplexing (OFDM) based systems. OFDM-based systems are very sensitive to frequency offset errors, and are characterized by producing high peak-to-average power ratio (PAPR) values. The IPLCP is evaluated in terms of average inter-carrier interference power, average signal to interference power, PAPR, and bit error rate. Theoretical and numerical simulations show that the IPLCP pulse performs well in OFDM-based systems in comparison to other existing pulses.

Keywords Inter-carrier interference (ICI) · Nyquist's first criterion · Orthogonal frequency division multiplexing (OFDM) · Peak-to-average power ratio (PAPR) · Pulse-shaping

1 Introduction

Orthogonal frequency division multiplexing (OFDM) is a bandwidth-efficient communication technique that has been widely used in several wireless communications standards; such as digital terrestrial TV broadcasting (DVB-T), Long Term Evolution (LTE) Advanced, Wireless Fidelity (WiFi), Wireless Personal Area Network (WPAN), and Worldwide Interoperability for Microwave Access (WiMAX) [1–4]. Further, OFDM-based systems are being studied and proposed as one of the key techniques to be implemented at the physical layer of 5G systems [5–8]. Furthermore, OFDM-based systems, combined

✉ Cesar A. Azurdia-Meza
cazurdia@ing.uchile.cl

[1] Department of Electrical Engineering, University of Chile, Santiago, Chile

[2] Department of Electrical Engineering, University of Santiago de Chile, Santiago, Chile

with multiple-input multiple-output (MIMO) techniques, are being suggested as the key technologies to be used at the physical layer of 5G cellular networks. The extensive use of OFDM-based systems is due to various advantages; such as, high data rate transmission capability, robustness to multi-path fading given by the ability to convert a frequency selective fading channel into several nearly flat fading channels, high bandwidth efficiency, and the use of guard intervals to deal with the effect of delay spread [1, 2]. But despite of all of the benefits offered by OFDM-based systems, there are certain technical issues that need to be addressed. OFDM-based systems are characterized by having high PAPR values [1, 2, 9], as it can be depicted in Fig. 2. Furthermore, OFDM-based systems are very sensitive to frequency offset errors caused by frequency differences between the local oscillators in the transmitter and the receiver, Doppler spread, and distortions within the channel, among others [1, 2, 10, 11]. Furthermore, carrier frequency offset causes a number of impairments, such as attenuation or rotation of subcarriers and inter-carrier interference (ICI) between them, increasing the error probability rate as the offset increases.

The power amplifier of a mobile terminal that implements OFDM-based systems has to accommodate higher PAPR values than prior standards, such as WCDMA, CDMA, and EDGE [9, 12]. As a result, PAPR plays and important role in the design of wireless communication systems because power amplifiers are usually operated in the linear mode rather than the saturation mode. A band-limited signal with high PAPR requires a large back-off to guarantee that the power amplifier operates inside its linear region to guarantee that the transmitted signal will not be distorted [9, 13–15]. In addition, signals with high PAPR require higher dynamic ranges of digital-to-analog converters (DAC) at the power amplifier. The total PAPR at the transmitter side is determined by the combination of the modulation scheme and the pulse shaping filter implemented [9, 13, 16]. Therefore, current ongoing research has focused on the design of a power amplifier that maintains high efficiency for signals with high PAPR. Several newly proposed power amplifiers have the potential to work with high PAPR signals, such as Doherty amplifiers [9, 12, 17], but at the moment these technologies are at an experimental stage. Hence, several methods for reducing PAPR in OFDM-based systems have been proposed; such as pre-coding methods [2, 4], probabilistic algorithms [9, 18], and non-linear expanding and compressing methods [9, 18].

Similarly, a number of methods have been developed to reduce the sensitivity to frequency offset, including windowing at the receiver side, pilot insertion, frequency domain equalization, and ICI self-cancellation schemes [1, 2, 4, 19]. The use of Nyquist-I pulses to reduce the ICI power in OFDM-based systems has been studied, proposed, and implemented by several scholars [10, 11, 19]. Pulses such as the raised cosine (RC) pulse, 'better than' raised cosine (BTRC) pulse [20], sinc power (SP) pulse [21], improved sinc power (ISP) pulse [22], new windowing function (NW) [23], and the phase modified sinc pulse (PM) [24] have been proposed, among others. The ISP pulse is characterized by having two design parameters, whereas the PM and NW have four. At the moment, the NW and PM are arguably the pulses that best diminish the effects of frequency offset in OFDM-based systems. But as error-free communication links and higher data rates will be demanded in next-generation networks, the design and implementation of new families of Nyquist-I pulses will become a fundamental research topic in the upcoming years.

In Arraño and Azurdia-Meza [25], a new family of Nyquist-I pulses, named improved parametric linear combination pulse (IPLCP), was proposed to reduce ICI power in OFDM-based systems. The IPLCP is characterized by having two new design parameters, giving extra degrees of freedom to reduce ICI for a certain roll-off factor. In this work, we analyse the performance of the IPLCP pulse applied to OFDM-based systems in terms of ICI power, signal to interference (SIR) power, PAPR, and bit error rate (BER). The

performance of the IPLCP pulse will be compared to those of other existing Nyquist-I pulses using numerical simulations and theoretical expressions. In this work, unless otherwise stated, the roll-off factor, α, is equal to 0.22, as suggested by the 3rd Generation Partnership Project (3GPP) for the pulse-shaping filter to be implemented at the transmitter side of the base station (BS) and user equipment (UE) [26, 27].

This paper has the following organization. A generic OFDM-based system model is introduced in Sect. 2. Whereas Sect. 3 examines the IPLCP family of Nyquist pulses. In Sect. 4 we analyse the performance of the IPLCP pulse by using theoretical expressions, and by implementing a real OFDM-based system via numerical simulations. We evaluate the performance of the IPLCP in terms of ICI power, SIR power, PAPR, and BER. Finally, conclusions are presented in Sect. 5.

2 OFDM System Model

An OFDM symbol is formed by the sum of N different data symbols (M-PSK, M-QAM, or other type of digital modulation), each transmitted on a different orthogonal subcarrier. The complex envelope of the transmitted OFDM symbol with pulse shaping is expressed as [24, 25]

$$s(t) = \mathrm{Re}\left\{ e^{j2\pi f_c t} \sum_{k=0}^{N-1} p(t) d_k e^{j2\pi f_k t} \right\}, \tag{1}$$

where j is the imaginary unit, d_k represents the k-th data symbol (which should not be confused with the OFDM symbol), N is the number of subcarriers implemented in the system, f_k is the k-th subcarrier frequency, f_c is the central carrier frequency, and $p(t)$ is the pulse-shaping function that limits or narrows each data symbol in a certain interval of time. A simplified scheme of an OFDM-based transceiver is shown in Fig. 1.

For the system shown in Fig. 1, we assume that the input data symbols are uncorrelated, where $\{d_k\}$ is a zero-mean independent sequence of unit variance and normalized symbol energy, and it is given as

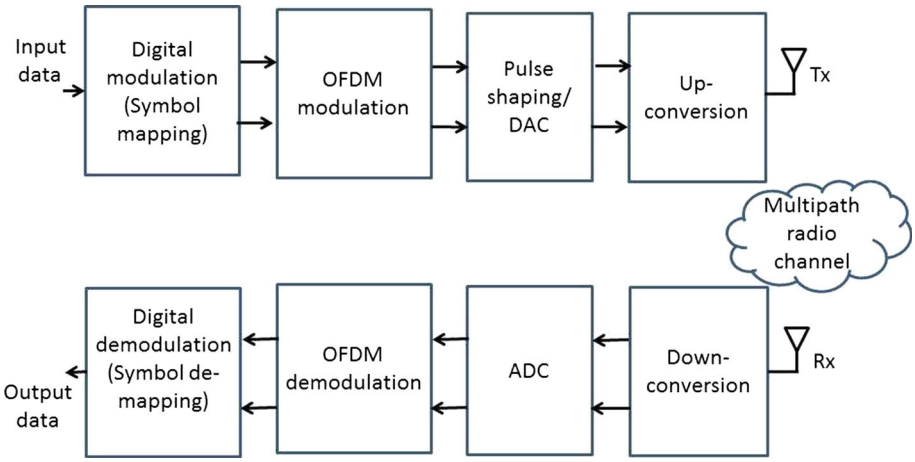

Fig. 1 General scheme of an OFDM transceiver

$$E[d_k d_m^*] = \begin{cases} 1, & \text{if } k = m \\ 0, & \text{if } k \neq m. \end{cases} \tag{2}$$

One very important characteristic of an OFDM-based system is the fact that the subcarriers must be orthogonal between them. To ensure orthogonality the following relationship must be true

$$f_k - f_m = \frac{k-m}{T}, \quad (k,m) \in \{0,1,\ldots,N-1\}, \tag{3}$$

where $1/T$ is the minimum required subcarrier frequency spacing to satisfy orthogonality. Therefore, individual subcarrier frequencies can be defined as

$$f_k = \frac{k}{T} \quad \forall k \in \{0,1\ldots,N-1\}. \tag{4}$$

Frequency offset, Δf, and phase error, θ, in OFDM-based systems are introduced due to channel distortion, and desynchronization between the crystal oscillator of the transmitter and receiver. The received signal is given by [20]

$$r(t) = e^{2\pi(\Delta f)t+\theta} \sum_{k=0}^{N-1} d_k p(t) e^{j2\pi f_k t}. \tag{5}$$

For the transmitted symbol d_m, the decision variable is given as [21]

$$\hat{d}_m = \int_{-\infty}^{\infty} r(t) e^{-j2\pi f_m t} \mathrm{d}t, \tag{6}$$

which could be decomposed into [22]

$$\hat{d}_m = d_m e^{j\theta} P(-\Delta f) + e^{j\theta} \sum_{\substack{k=0 \\ k\neq m}}^{N-1} d_k P\left(\frac{m-k}{T} - \Delta f\right). \tag{7}$$

The power of the desired signal can be calculated as

$$\sigma_m = |d_m|^2 |P(\Delta f)|^2, \tag{8}$$

and the ICI power is given as follows [28]

$$\sigma_{ICI}^m = \sum_{\substack{k=0 \\ k\neq m}}^{N-1} \sum_{\substack{n=0 \\ n\neq m}}^{N-1} d_k d_n^* P\left(\frac{k-m}{T} + \Delta f\right) P\left(\frac{n-m}{T} + \Delta f\right). \tag{9}$$

Considering (2) and (9), the average ICI power is given by

$$\overline{\sigma_{ICI}^m} = \sum_{\substack{k=0 \\ k\neq m}}^{N-1} \left| P\left(\frac{k-m}{T} + \Delta f\right) \right|^2. \tag{10}$$

Notice that the ICI power mainly depends on the value of the frequency offset Δf and the pulse-shaping function $P(f)$, which is the main reason it is so important to choose the right pulse-shaping function for the OFDM-based system. The ratio of average signal power, $|P(\Delta f)|^2$, to average ICI power is denoted as SIR, and it is expressed as follows [23, 24]

$$SIR = \frac{|P(\Delta f)|^2}{\sum\limits_{\substack{k=0 \\ k\neq m}}^{N-1} |P((k-m)/T + \Delta f)|^2}. \tag{11}$$

Similarly to the average ICI power, the expression given by (11) depends on the frequency offset, Δf, and the pulse shaping function $P(f)$.

3 Improved Parametric Linear Combination Pulse

Based on the fact that each data symbol of an OFDM-based system is transmitted on a different subcarrier, the signal analysis cannot be made in the time domain, because the envelope given by (1) is the result of the sum of N orthogonal signals. The time-domain signal given by (1) does not provide much information regarding the behavior of the digital data, as seen in Fig. 2. In Fig. 2 we simulated an OFDM-based system according to the IEEE 802.11a specifications [3, 29], and plotted its time-domain signal. We cannot ensure that the subcarriers really satisfy (3), fact that could produce interference between subcarriers, resulting in information losses.

Alternatively, the analysis of an OFDM-based system is normally done in the frequency domain, where the measure of interference between data is given by the ICI power instead of the inter symbol interference (ISI). Graphically, and in its most simplified way, the spectrum of an OFDM signal is mainly the Fourier transform of the Nyquist pulse shaping filter $p(t)$, previously defined in Sect. 2 as $P(f)$, placed on the frequency of each subcarrier, as seen in Fig. 3. Hence, to achieve zero interference between subcarriers, $P(f)$ has to behave as a Nyquist-I pulse. This can be derived by using Eqs. (1) and (3), leading to the following expression [20]

$$\int_{-\infty}^{\infty} p(t) e^{j2\pi(f_k - f_m)t} \mathrm{d}t = \begin{cases} 1, & \text{if } k = m \\ 0, & \text{if } k \neq m, \end{cases} \tag{12}$$

which indicates that $P(f)$ should have spectral null points at the frequencies $\pm 1/T, \pm 2/T, \ldots$ to ensure subcarrier orthogonality. Formally this could be expressed as

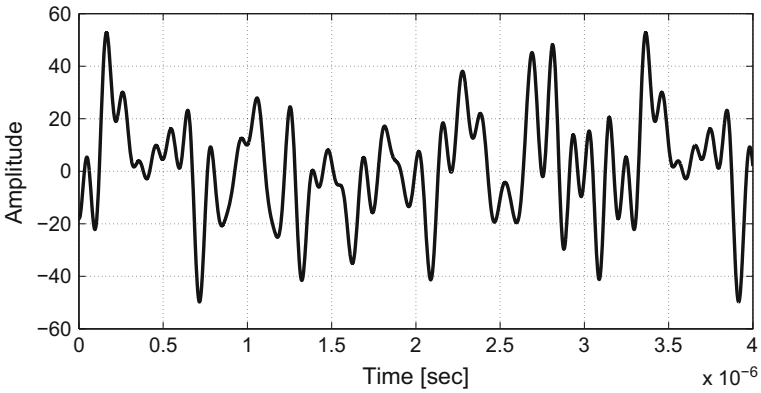

Fig. 2 OFDM time-domain signal based on IEEE 802.11a specifications

$$P(f) = \begin{cases} 1, & \text{if } f = 0 \\ 0, & \text{if } f = \pm 1/T, \pm 2/T, \ldots, \end{cases} \tag{13}$$

which is basically Nyquist's first criterion, but written in the frequency domain.

The frequency domain expression of the IPLCP was originally derived in [25], and it is given as follows

$$P_{IPLCP}(f) = e^{\left(-\varepsilon\pi^2(fT)^2\right)} \times \left[\frac{\sin(\pi fT)}{\pi fT} \times \left[\frac{4(1-\mu)\sin^2(\pi\alpha fT/2)}{\pi^2\alpha^2(fT)^2} + \frac{\pi\alpha\mu fT\sin(\pi\alpha fT)}{\pi^2\alpha^2(fT)^2}\right]\right]^{\gamma}, \tag{14}$$

where μ corresponds to the linear combination constant, and it is defined for all real numbers. This constant adds an additional degree of freedom for a given roll-off factor α, which is the only independent variable in pulses like the RC or the BTRC. The roll-off factor α is defined for $0 \leq \alpha \leq 1$. Notice that the IPLCP is equivalent to the γ-th power of the PLCP pulse [13] multiplied by the exponential factor $\exp(-\varepsilon\pi^2(fT)^2)$. There are two extra degrees of freedom added: γ and ε, both defined for all real numbers. To prove that the IPLCP meets the Nyquist-I criterion, given in (13), lets notice that (14) evaluated for $f = 0$ and for any value of α, μ, ε or γ, is always equal to one. Additionally, the IPLCP pulse, evaluated for $f = \pm 1/T, \pm 2/T, \ldots$, is always equal to zero. Therefore, the IPLCP fulfills Nyquist's first criterion.

To analyse the effect that the parameters ε and γ have on the pulse-shaping function, only one parameter is varied while the other one is fixed. We have also fixed the value of the parameter μ equal to 1.6 to be consistent with related work [13, 25]. As seen in Fig. 4, if the value of ε increases, the sidelobes of the IPLCP frequency function are considerably reduced without significantly affecting the central lobe width. In Fig. 5 it can be noticed that in the time domain, as ε increases, the rectangular behaviour is almost maintained; therefore, by increasing the value of ε, an important ICI and SIR power reduction would be achieved without considerably affecting the time domain performance.

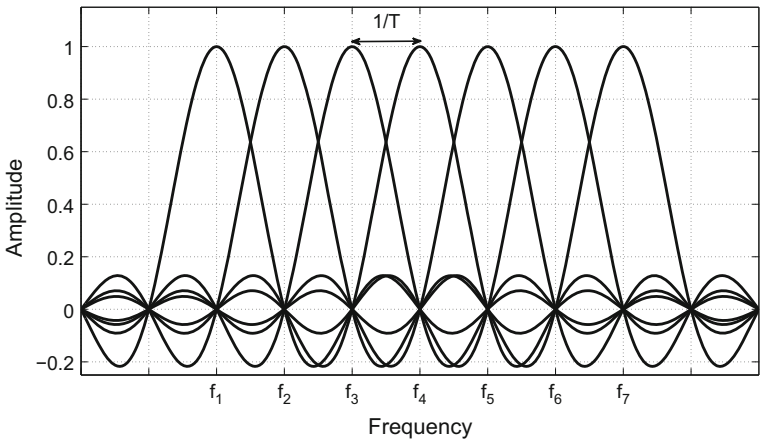

Fig. 3 Simplified graph of the spectrum of an OFDM-based system

On the other hand, if one fixes the value of ε and increases γ, the sidelobes are rapidly reduced, but the central lobe width is narrower, as seen in Fig. 6. A pulse with a narrow central lobe and almost no sidelobes (similar to a delta Dirac function) highly reduces the ICI power, but on the other hand, increases the BER of the system because the synchronization between the oscillator of the transmitter and the receiver need to be almost perfect to recover the desired signal [22, 25]. As shown in Fig. 7, the time domain behavior is not preserved as γ increases, hence the time domain function of the IPLCP looks more like a triangle. Therefore, the pulse is not able to effectively limit the symbol duration period. Further, its amplitude is considerably reduced, attenuating the data symbols and increasing the BER.

The frequency and time-domain responses of the IPLCP, as well as for other pulses, are illustrated in Figs. 8 and 9, respectively. For comparison purposes, the design parameters used in this paper for the SP [23], ISP [24], NW [23], and PW [23] pulses are the ones that provide the best performance in OFDM-based systems. Therefore, we compare the IPLCP with the SP, ISP, NW, and PW pulses. As previously indicated, we fixed the value of the constant μ equal to 1.6, and through extensive computer simulations we found the sub-optimum values of ε and γ equal to 0.1 and 1, respectively. In general there is an optimum μ, ε, and γ for every roll-off factor and transmission scheme, although they might not be unique. From inspection of Fig. 8, it can be seen that the IPLCP has a similar frequency response to the SP, ISP, and PM pulses. Further, the relative magnitudes of the two largest sidelobes of the previous pulses behave similarly. To reduce the PAPR and ICI power of the signals to be transmitted, we should design a Nyquist pulse with a reduced tail size because the relative magnitudes of the two largest sidelobes are the ones that have the biggest effect on the PAPR and ICI [9, 13, 30, 31]. In the case of the NW pulse, even though its frequency response decays faster, it possesses a narrow central lobe (similar to a delta Dirac function); therefore, an increase in the average BER is expected [22, 25]. Regarding the time responses of the evaluated pulses, depicted in Fig. 9, it can be seen that the IPLCP, SP, ISP, and PM pulses have a similar response. Whereas, the time response of the NW pulse is not preserved; hence, the NW pulse is not able to effectively limit the OFDM symbol period duration [25]. Further, its amplitude is considerably reduced, attenuating the data symbols and increasing the BER.

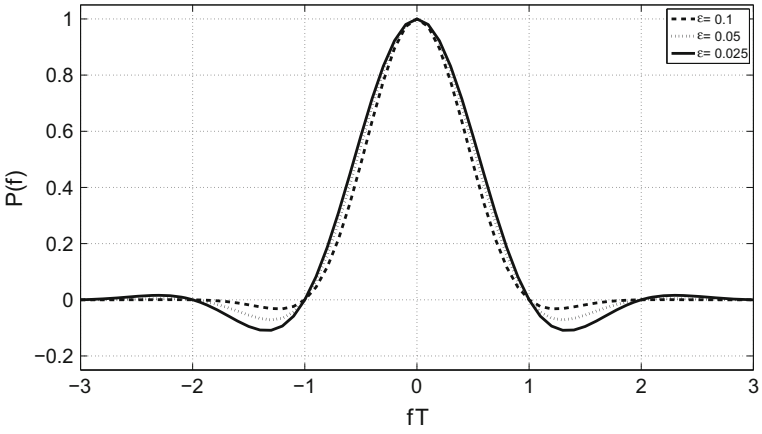

Fig. 4 Frequency functions of the IPLCP as ε varies for $\alpha = 0.22$, $\mu = 1.6$, and $\gamma = 1$

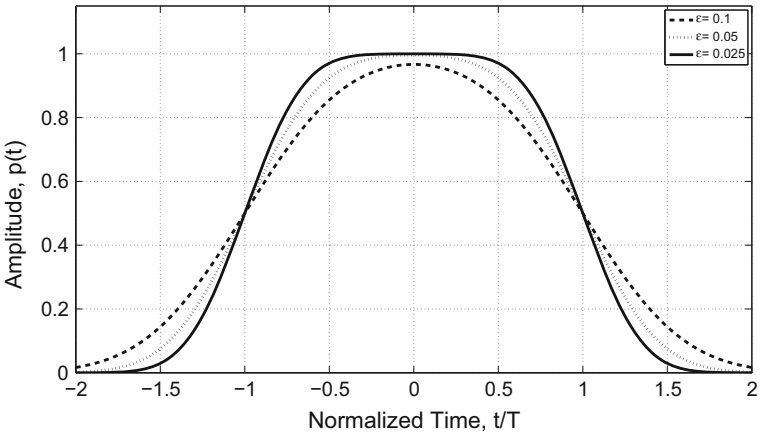

Fig. 5 Time-domain functions of the IPLCP as ε varies for $\alpha = 0.22$, $\mu = 1.6$, and $\gamma = 1$

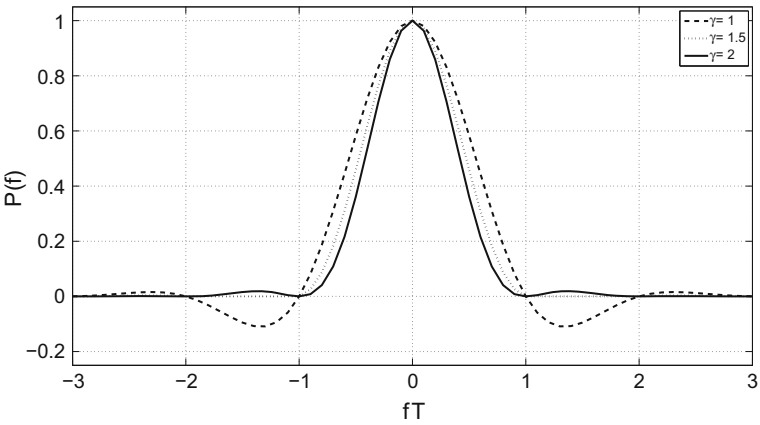

Fig. 6 Frequency functions of the IPLCP as γ varies for $\alpha = 0.22$, $\mu = 1.6$, and $\varepsilon = 0.1$

4 Performance Evaluation

In this work, we evaluate the efficiency of the IPLCP pulse in OFDM-based systems and compare its performance with other existing pulses; such as the SP, ISP, NW, and PM. Theoretical and numerical simulations are shown to verify that the IPLCP performs well compared to the SP, ISP, NW and PW pulses. Sub-optimum design parameters were used to evaluate the previous pulses, as indicated in Sect. 3. A real OFDM-based simulation scenario was used to validate the theoretical results. Table 1 illustrates the parameters implemented in the simulations.

First, we evaluate the ICI power of the IPCLP and the other pulses by simulating a 64 subcarrier OFDM-based system using binary phase shift keying (BPSK) digital modulation. In Fig. 10, we plotted the ICI power of the different pulse-shaping functions applied to a 64 subcarrier OFDM-based system. It can be seen that for a normalized frequency offset higher or equal to approximately 0.15, the ICI power of the evaluated pulse shaping

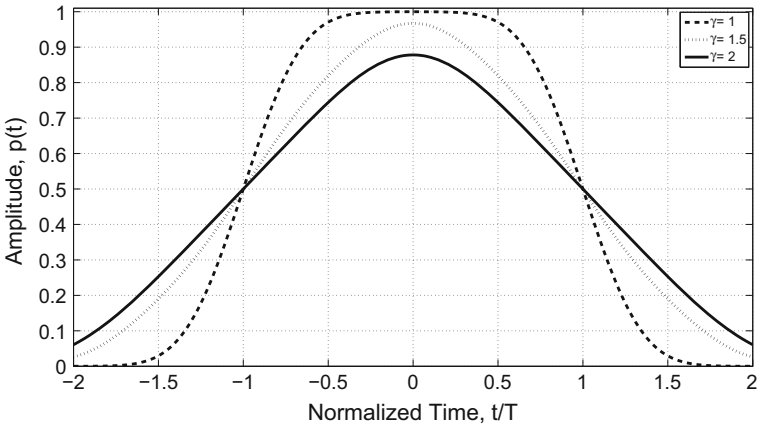

Fig. 7 Time-domain functions of the IPLCP as γ varies for $\alpha = 0.22$, $\mu = 1.6$, and $\varepsilon = 0.1$

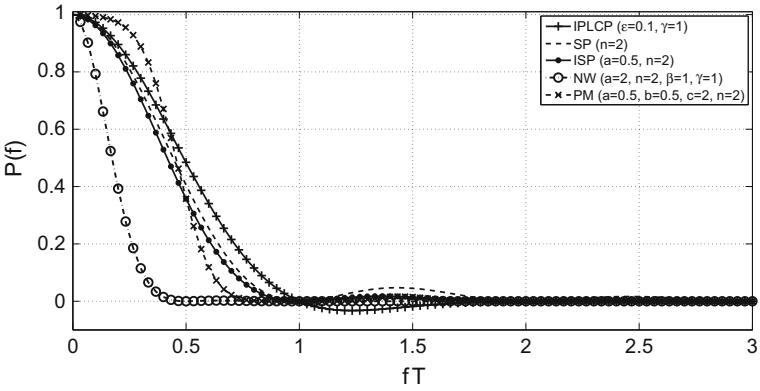

Fig. 8 Frequency responses of the IPLCP with $\mu = 1.6$ and other existing pulses for an excess bandwidth $\alpha = 0.22$

functions is the same. For normalized frequency offsets <0.15, the NW pulse outperforms the other pulses, whereas the IPLCP pulse performs similarly to the rest of the pulses. It can be seen that for a normalized frequency offset equal to 0.05, the NW pulse possesses an ICI power equal to −49 dB, whereas the IPLCP has an ICI power equal to −46.2 dB. Overall, as the normalized frequency offset diminishes, ICI power is reduced considerably. Similarly, it can be seen in Fig. 11 that the NW function outperforms the other pulses in terms of SIR power, and for small normalized frequency offsets, the NW function outperforms the other pulses. For larger normalized frequency offsets, the trend is similar for all of the pulses in terms of SIR power. In general, we can conclude that the NW function outperforms the rest of the pulses in terms of ICI and SIR power because its frequency response decays faster than the other pulses, as depicted in Fig. 8 [20, 21, 24, 30]. It can be seen in Fig. 8 that the NW pulse possesses the smallest sidelobes compared to the other evaluated pulses. Larger sidelobes will make the pulse more sensitive to ICI and SIR. According to (10), the average ICI power of the *m*th symbol depends on the number of

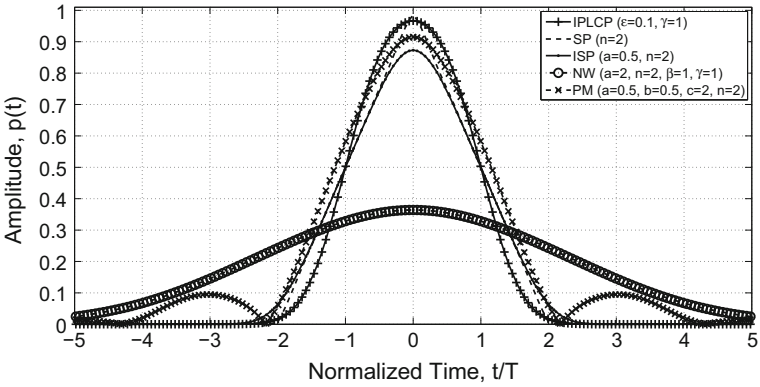

Fig. 9 Time response of the IPLCP with $\mu = 1.6$ and other existing pulses for an excess bandwidth $\alpha = 0.22$

subcarriers, and on the spectral magnitudes of the pulse-shaping function at the frequencies $((k-m)/T) + \Delta f,\ k \neq m,\ k = 0, 1, \ldots, N-1$. Similarly, as can be depicted in (11), the average SIR power of the mth symbol depends on the number of subcarriers, and on the spectral magnitudes of the pulse-shaping function implemented. Therefore, a pulse with small sidelobes is desired to diminish the effects of ICI and maximize the SIR power. Even though the NW pulse performs well in terms of ICI and SIR power, it possesses a narrow central lobe that will increase the BER of the system.

The total PAPR at the transmitter side is determined by the combination of the pulse shaping function and the technology implemented, in this case an OFDM-based system [9, 13, 32]. To evaluate the PAPR of individual system configurations, we simulated the transmission of 10^5 system blocks, 256 subcarriers, and 16-QAM digital modulation was implemented. After calculating the PAPR of each block, the data was presented as an empirical complementary distribution function (CCDF), which measures the probability that the transmitted signal's PAPR exceeds a certain threshold defined as $PAPR_0$, $\Pr\{PAPR > PAPR_0\}$ [4, 9, 13]. As done in [9, 13, 32], the PAPR was measured and analysed after filtering the OFDM signal with the proposed IPLCP pulse and the other evaluated pulses; therefore, the Nyquist pulses were used as matched filters. In Fig. 12 we plotted the PAPR of the different pulses applied in a 256 subcarrier OFDM-based system. It can be seen that the IPLCP pulse achieved the lowest $PAPR_0$ among the evaluated pulses. For example, for a probability of 10^{-4}, the IPLCP has a $PAPR_0$ equal to 12.32 dB,

Table 1 OFDM system simulation parameters

Parameter	Value
Modulation	BPSK, 16-QAM
Number of subcarriers	64, 256
Input data block size	52, 64
Transmission bandwidth	20 MHz
Block oversampling	4
Signal-to-noise ratio	30 dB
Roll-off factor	$\alpha = 0.22$

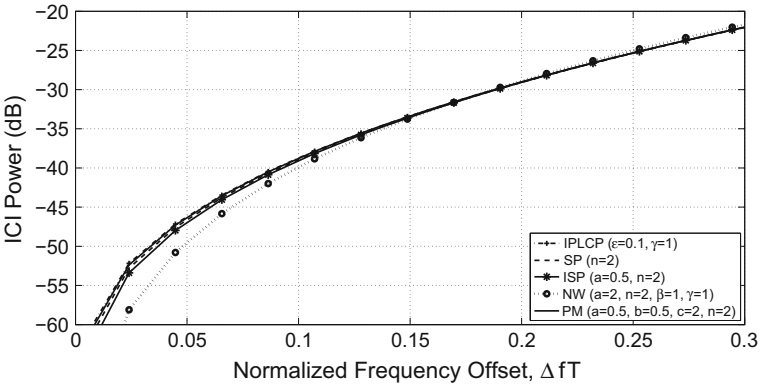

Fig. 10 ICI power of different pulse shaping functions applied in a 64 subcarrier OFDM-based system

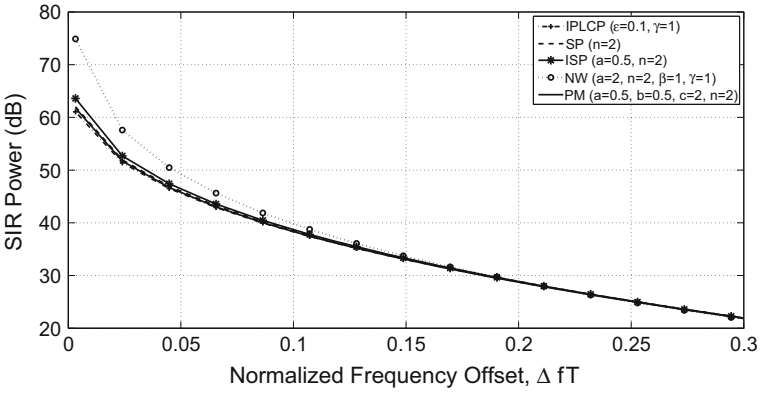

Fig. 11 SIR power of different pulse shaping functions applied in a 64 subcarrier OFDM-based system

whereas the SP, ISP, PM and NW pulses have a $PAPR_0$ equal to 13.45, 13.67, 14.65, and 14.89 dB, respectively. Compared to the NW pulse, the IPLCP has a gain of 2.32 dB for a probability of 10^{-4}. The trend is the same for other probability values.

Yielding small ICI power, maximizing SIR power, and diminishing PAPR are not the only evaluation metrics to be considered in the design of an optimal pulse shaping filter in OFDM-based systems. The most important evaluation metric in any digital communication scheme is the BER, as it plays an important role in assessing the performance and effectiveness of an OFDM-based communication system. To evaluate the BER of the IPLCP and the other pulses, we used the theoretical expression derived in [10]. This theoretical expression is used to compare the BER of different pulse shaping functions assuming an additive white Gaussian noise (AWGN) channel and BPSK modulation. The average BER is given as a function of the carrier phase noise θ, average ICI power (P_{ICI}), carrier frequency offset Δf, and the pulse shaping function $P(f)$. The average BER is given as follows [10]

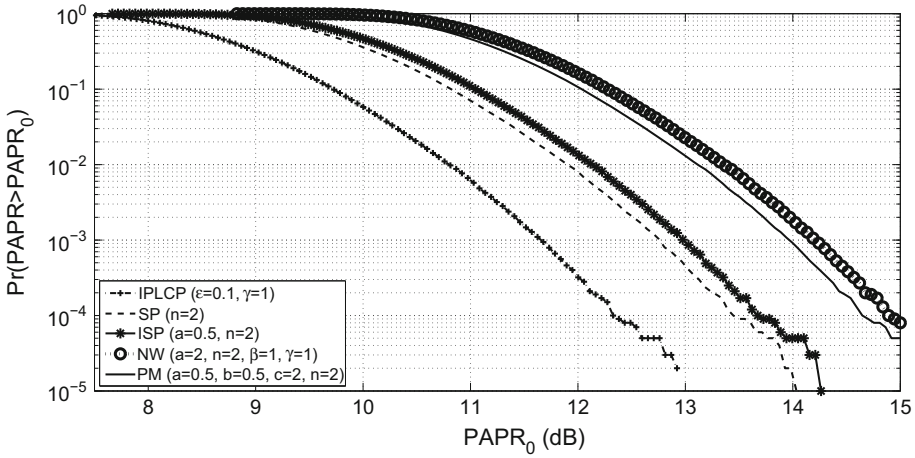

Fig. 12 CCDF of PAPR for different pulse shaping functions applied in a 256 subcarrier OFDM-based system

$$BER_{OFDM} = 1 - (1 - OFDM_{symbol})^{N}, \tag{15}$$

where N represents the number of subcarriers or symbols per modulated block. Further, the BER of an BPSK-OFDM symbol is given as follows [10]

$$\begin{aligned} BER_{symbol} = \frac{1}{2}\Big(&Q\Big\{\cos\theta\big[P(-\Delta f) + \sqrt{P_{ICI}}\big]\sqrt{2\gamma_b}\Big\} \\ &+Q\Big\{\cos\theta\big[P(-\Delta f) - \sqrt{P_{ICI}}\big]\sqrt{2\gamma_b}\Big\}\Big), \end{aligned} \tag{16}$$

where $\gamma_b = E_b/N_0$. If the spectral sidelobes of the pulse shaping functions are very small in comparison to its main lobe, as it was previously analysed in Fig 8, then (16) can be approximated as [10]

$$BER_{symbol} \approx Q\Big[\cos(\theta)P(-\Delta f)\sqrt{2\gamma_b}\Big]. \tag{17}$$

Therefore, in this work the BER of the proposed system is evaluated using the expression given in (17). We evaluated the BER of the proposed system using a frequency offset Δf equal to 0.3, and a carrier phase noise of $\theta = 10^\circ$ and $\theta = 30^\circ$. In general, we achieved a lower BER by using a smaller carrier phase noise angle, in accordance with the expression given in (17). In Fig. 13, we plotted the BER of the BPSK-OFDM system with $\theta = 10^\circ$, whereas, in Fig. 14, we plotted the BER with $\theta = 30^\circ$. As seen in both scenarios, the NW pulse performs poorly. Whereas, the IPLCP is the pulse with the second best BER performance in both scenarios. Interestingly, the NW pulse performs poorly in both scenarios. This is because it possesses a narrow central lobe (similar to a delta Dirac function), as depicted in Fig. 8. This increases the BER of the system because the oscillators of the transmitter and the receiver need to be perfectly synchronized to recover the desired signal without errors. It can be seen in Fig. 8 that the PM pulse possesses the most broaden central lobe compared to those of the other evaluated pulses, as well as small sidelobes; therefore, yielding the smallest BER within the evaluated pulses [10].

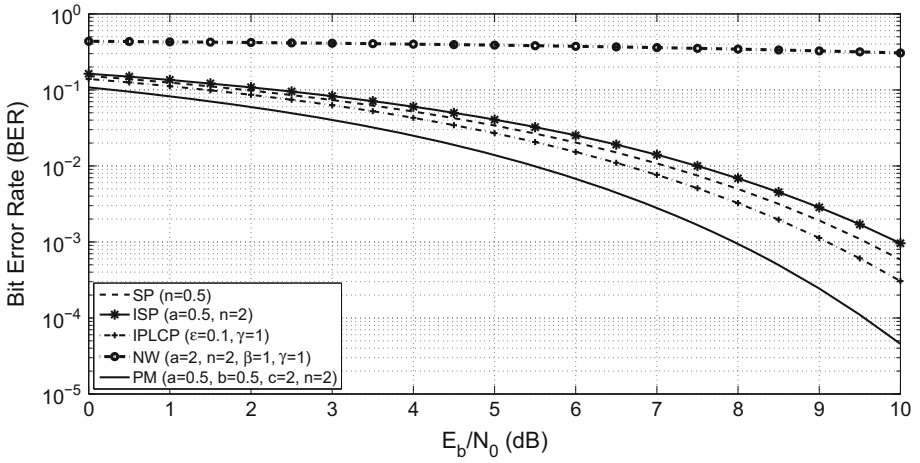

Fig. 13 BER evaluation for different pulse shaping functions using a BPSK-OFDM system with $\Delta f = 0.3$ and $\theta = 10^\circ$

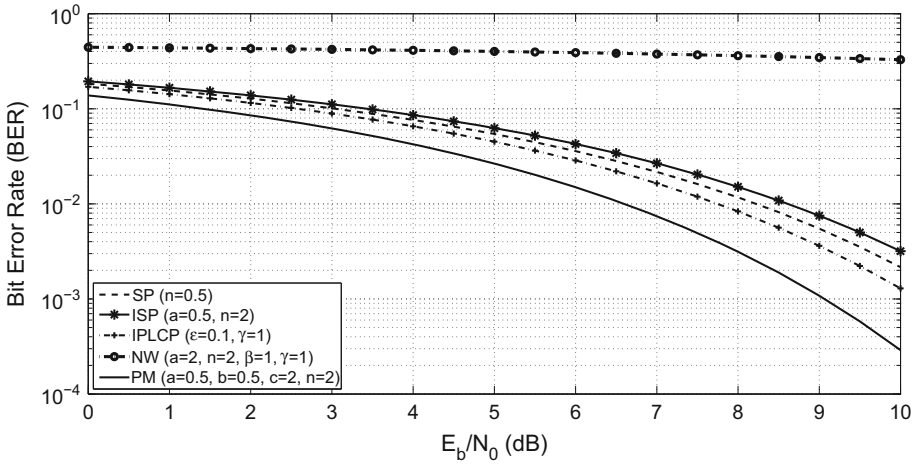

Fig. 14 BER evaluation for different pulse shaping functions using a BPSK-OFDM system with $\Delta f = 0.3$ and $\theta = 30^\circ$

Overall, the sub-optimum IPLCP performs well in OFDM-based systems for different evaluation metrics. Through extensive computer simulations it was found that the sub-optimum IPLCP performs well using $\varepsilon = 0.1$, $\gamma = 1$, $\mu = 1.60$, and $\alpha = 0.22$ for reducing ICI and PAPR power, maximizing SIR, and diminishing BER.

5 Conclusion

In this work, the IPLCP pulse was evaluated in OFDM-based systems in terms of ICI power, SIR power, PAPR and, BER. For a roll-off factor $\alpha = 0.22$, the sub-optimum values of the constants ε and γ are equal to 0.1 and 1, respectively. Simulations showed that the

IPLCP pulse provided the lowest PAPR in comparison to the other evaluated pulses. The NW pulse shaping function had the best performance in terms of ICI and SIR power, but at the expense of a poor BER performance. Whereas, the other pulse shaping functions performed similarly in terms of ICI and SIR power, e.g., there is <1 dB difference between the evaluated pulse shaping functions for low Δf values. The IPLCP performed well in terms of average BER, only outperformed by the PM pulse shaping function. Overall, the sub-optimum IPLCP pulse performed well in our simulation scenarios.

Acknowledgments The authors acknowledge the financial support of the Program U-INICIA VID 2014, Grant No. UI-02/2014, University of Chile. The authors also acknowledge the partial financial support of the Project FONDECYT 11121655 and the "Center for Multidisciplinary Research on Signal Processing" (CONICYT/ACT1120 Project).

References

1. Hwang, T., Yang, C., Wu, G., Li, S., & Li, G. Y. (2009). OFDM and its wireless applications: A survey. *IEEE Transactions on Vehicular Technology*, *58*(4), 1673–1694.
2. Nee, R., & Prasad, R. (2000). *OFDM wireless multimedia communications*. Norwood: Artech House.
3. Walke, B. H., Mangold, S., & Berlemann, L. (2006). *IEEE 802 wireless systems: Protocols, multi-hop mesh/relaying, performance and spectrum coexistence*. New York: Wiley.
4. Prasad, R. (2004). *OFDM for wireless communications systems*. Norwood: Artech House.
5. Roh, W., Seol, J. Y., Park, J. H., Lee, B. H., Lee, J. K., Kim, J. S., et al. (2014). Millimeter-wave beamforming as an enabling technology for 5G cellular communications: Theoretical feasibility and prototype results. *IEEE Communications Magazine*, *52*(2), 106–113.
6. Rappaport, T. S., Sun, S., Mayzus, R., Zhao, H., Azar, Y., Wang, K., et al. (2013). Millimeter wave mobile communications for 5G cellular: It will work!. *IEEE Access*, *1*, 335–349.
7. Chen, S., & Zhao, J. (2014). The requirements, challenges, and technologies for 5G of terrestrial mobile telecommunication. *IEEE Communications Magazine*, *52*(5), 36–43.
8. Daniels, R. C., Murdock, J. N., Rappaport, T. S., & Heath, R. W. (2010). 60 GHz wireless: Up close and personal. *IEEE Microwave Magazine*, *11*(7), 44–50.
9. Azurdia-Meza, C. A., Lee, K. J., & Lee, K. S. (2012). PAPR reduction by pulse shaping using Nyquist linear combination pulses. *IEICE Electronics Express*, *9*(19), 1534–1541.
10. Le, K. N. (2008). Insights on ICI and its effects on performance of OFDM systems. *Digital Signal Processing*, *18*(6), 876–884.
11. Tan, P., & Beaulieu, N. (2009). Analysis of the effects of Nyquist pulse-shaping on the performance of OFDM systems with carrier frequency offset. *European Transactions on Telecommunications*, *20*(1), 9–22.
12. Choi, J., Kang, K., Kim, K., Park, J., Jin, B., & Kim, B. (2009). Power amplifiers and transmitters for next generation mobile headsets. *Journal of Semiconductor Technology and Science*, *9*(4), 249–256.
13. Azurdia-Meza, C. A., Lee, K., & Lee, K. (2012). PAPR reduction in SC-FDMA by pulse shaping using parametric linear combination pulses. *IEEE Communications Letters*, *16*(12), 2008–2011.
14. Myung, H. G., Lim, J., & Goodman, D. J. (2006). Single carrier FDMA for uplink wireless transmission. *IEEE Vehicular Technology Magazine*, *1*(3), 30–38.
15. Myung, H. G., Lim, J., & Goodman, D. (2006). Peak-to-average power ratio of single carrier FDMA with pulse shaping. In *IEEE 17th international symposium PIMRC*.
16. Azurdia-Meza, C. A. (2013). PAPR reduction in SC-IFDMA uplink system using parametric pulses. In *IEEE Latin-America conference on communications*.
17. Berglund, B., Johansson, J., & Lejon, T. (2006). High efficiency power amplifiers. *Ericson Review*, *83*(3), 92–96.
18. Lei, L., Enchang, S., & Yanhua, Z. (2010). A method for PAPR reduction using pilot sequences in SC-FDMA.' In *6th international conference WiCom*.
19. Mohanty, S., & Das, S. (2008). A comparative study of pulse shaping functions for ICI power reduction in OFDM system. In *Annual IEEE India conference* (pp. 312–316). IEEE.
20. Beaulieu, N. C., & Tan, P. (2004). Reduced ICI in OFDM systems using the "better than" raised-cosine pulse. *IEEE Communications Letters*, *8*(3), 135–137.

21. Mourad, H. M. (2007). Reducing ICI in OFDM systems using a proposed pulse shape. *Wireless Personal Communications*, *40*(1), 41–48.
22. Kumbasar, V., & Kucur, O. (2007). ICI reduction in OFDM systems by using improved sinc power pulse. *Digital Signal Processing*, *17*(6), 997–1006.
23. Yadav, P. K., Dwivedi, V. K., Karwal, V., & Gupta, J. P. (2014). A new windowing function to reduce ICI in OFDM systems. *International Journal of Electronics Letters*, *2*(1), 2–7.
24. Alexandru, N. D., & Onofrei, A. L. (2010). ICI reduction in OFDM systems using phase modified sinc pulse. *Wireless Personal Communications*, *53*(1), 141–151.
25. Arraño, H. F., & Azurdia-Meza, C. A. (2014). ICI reduction in OFDM systems using a new family of Nyquist-I pulses. In *IEEE Latin-America conference on communications*.
26. Third Generation Partnership Project (3GPP). (2014). Universal mobile telecommunications system (UMTS). In *Base station BS radio transmission and reception FDD*. European Telecommunications Standards Institute, Technical Report 125.104.
27. 3rd Generation Partnership Project (3GPP). (2014). Universal mobile telecommunications system (UMTS). In *User equipment UE radio transmission and reception FDD*. European Telecommunications Standards Institute, Technical Report 125.101.
28. Tan, P., & Beaulieu, N. (2004). A novel pulse-shaping for reduced ICI in OFDM systems. In *IEEE 60th vehicular technology conference* (Vol. 1, pp. 456–459).
29. IEEE wireless LAN edition—A compilation based on IEEE Std. 802.11TM-199 (R2003) and its amendments, IEEE Std., Rev. R2003.
30. Farhang-Boroujeny, B. (2008). A square-root Nyquist M filter design for digital communication systems. *IEEE Transactions on Signal Processing*, *56*(5), 2127–2132.
31. Chatelain, B., & Gagnon, F. (2004). Peak-to-average power ratio and intersymbol interference reduction by Nyquist optimization. In *IEEE vehicular technology conference*.
32. Wei, Y. D., & Chen, Y. F. (2010). Peak-to-average power ratio PAPR reduction by pulse shaping using the K-exponential filter. *IEICE Transactions on Communications*, *E93–B*(11), 3180–3183.

Cesar A. Azurdia-Meza received the B.Sc. degree in electrical engineering from Universidad del Valle de Guatemala, Guatemala in 2005, and the M.Sc. degree in electrical engineering from Linnaeus University, Sweden in 2009. In 2013 he obtained the Ph.D. degree in Electronics and Radio Engineering, Kyung Hee University, Republic of Korea. He joined the Department of Electrical Engineering, University of Chile as an Assistant Professor in August 2013. He has served as Technical Program Committee (TPC) member for multiple conferences, as well as a reviewer in journals such as IEEE Communications Letter, IEEE Transactions on Wireless Communications, Wireless Personal Communications, EURASIP Journal on Advances in Signal Processing, and Telecommunication Systems. Dr. Azurdia is an IEEE Communications Society Member. His research interests include topics such as Nyquist's ISI criterion, OFDM-based systems, SC-FDMA, visible light communication systems, 5G and beyond enabling technologies, and signal processing techniques for communication systems.

Hernán F. Arraño received the B. Sc. Degree in Electrical Engineering from Universidad de Chile, Chile in 2014. Among his research projects, he was part of the team that built the first Chilean nanosatellite at the Faculty of Physics and Mathematical Sciences, Universidad de Chile. He is currently working as an assistant researcher at the Advanced Communications Laboratory, Department of Electrical Engineering, Universidad de Chile. His research interests include communication systems, multiple access techniques, OFDM, MIMO, multicarrier transmission schemes, and cellular systems.

Claudio Estevez received a B.S. in electrical and computer engineering from the University of Puerto Rico, Mayaguez, PR, USA, 2001; an M.S. in electrical and computer engineering with a minor in optical engineering from the University of Alabama in Huntsville, Huntsville, AL, USA, 2003; and a Ph.D. in electrical and computer engineering and with a minor in computer science from the Georgia Institute of Technology, Atlanta, GA, USA, 2010. In 2011, he was hired as an assistant professor by the electrical engineering department at Universidad de Chile. In 2012, he obtained a Chilean national research Grant (FONDECYT) to study MAC protocols in WPAN using 60 GHz. In the same year he was appointed coordinator of the Communication Networks M.Eng. Program. His research interests include: Connection-oriented transport protocols, network fairness study, MAC-layer protocols in WPAN, 60-GHz WPAN applications, cloud computing with data mining/warehousing, wireless body area networks, remote biological monitoring.

Ismael Soto was born in Punta Arenas, Chile. He received an Engineering degree from Universidad de Santiago de Chile in 1982, the Master of Engineering degree from University Federico Santa Maria in 1990, and the Ph.D. degree from the University of Staffordshire, U.K. in 1997. He has taught in the Department of Computer Science, Industrial Engineering, and Electrical Engineering, Universidad de Santiago de Chile. Currently he is an Associate Professor in Telecommunications and Signal Processing at the Electrical Engineering Department, University de Santiago de Chile. He has worked in wireless networking and security. Professor Ismael Soto has been the National Director and member of the Institute of Electrical and Electronics Engineers (IEEE Chilean Section), and member of the International Speech Communication Association. His main research interests are OFDMA, signal processing, coding, and equalization.